

Sharpening radiographs

(tomography reconstruction kernel/noise elimination)

K. T. SMITH[†], S. L. WAGNER[‡], AND M. J. BOTTEMA[†]

[†]Mathematics Department, Oregon State University, Corvallis, OR 97331; and [‡]Environmental Health, Good Samaritan Hospital, Corvallis, OR 97330

Communicated by Peter D. Lax, March 12, 1984

ABSTRACT This article describes a method for clarifying and sharpening radiographs. The method uses convolution with a computed tomography reconstruction kernel and a noise elimination procedure to control the noise amplification of the convolution. The effect is to flatten global variations and to sharpen and magnify local variations. Examples from industry and medicine are included.

Introduction

There are several reasons for the difficulty in reading radiographs. In addition to superposition, three main problems are as follows. (i) Signals due to features of interest are often very small relative to those due simply to thickness—on the order of 1/1000th for many soft tissue discriminations. (ii) Even if the x-ray attenuation coefficient is discontinuous at boundaries between tissues, the discontinuities are removed by the integration and averaging of the x-ray process. Radiographs seldom delineate edges. (iii) The same feature looks different in different locations—e.g., in a flat background or in a changing one.

The sharpening process is not image enhancement in the usual sense. It does not involve thresholding, computer decisions, edge detection, etc., but rather a specific mathematical property of the parallel beam x-ray transform

$$P_{\theta}f(x) = \int_{-x}^x f(x+t\theta)dt, \quad [1.1]$$

where θ is the x-ray direction, x is a point in θ^{\perp} (the subspace orthogonal to θ), and f is the x-ray attenuation coefficient of the object x-rayed. $P_{\theta}f(x)$ is the attenuation due to f along the line through x with direction θ .

Computed tomography provides a numerical approximation to the inverse transform (1)

$$f(x) = c \Lambda \int_{S^{n-1}} P_{\theta}f(E_{\theta}x)d\theta, \quad [1.2]$$

where E_{θ} is the orthogonal projection on θ^{\perp} , and Λ is defined via the Fourier transform by

$$(\Lambda g)^{\wedge}(\xi) = |\xi| \hat{g}(\xi). \quad [1.3]$$

Because of the singularity of Λ , it is customary to replace f by $e*f$, where e is an approximate δ -function, to obtain

$$e*f(x) = \int_{S^{n-1}} k*P_{\theta}f(E_{\theta}x)d\theta \quad k = c\Lambda P_{\theta}e. \quad [1.4]$$

The publication costs of this article were defrayed in part by page charge payment. This article must therefore be hereby marked "advertisement" in accordance with 18 U.S.C. §1734 solely to indicate this fact.



FIG. 1. Effect of convolution on ellipses. The function g (Upper left) is a large ellipse with small elliptical bumps (Lower left); $0.5g + 0.5k*g$ and $k*g$ are shown (Right).

In dimension 2 and with a particular approximate δ -function e , Eq. 1.4 is the famous reconstruction formula of Ramachandran and Lakshminarayanan (2). (e is called the point spread function, and k is called the reconstruction kernel.)

The mathematical property used in the sharpening is provided by the Logan–Shepp ellipse theorem (3).

ELLIPSE THEOREM. If f is the characteristic function of a 2-dimensional ellipse with projection $(-a, a)$ on the line θ^{\perp} , then

$$\Lambda P_{\theta}f(x) = c \begin{cases} 1 & |x| < a \\ 1 - |x|(x^2 - a^2)^{-1/2} & |x| > a \end{cases} \quad [1.5]$$

In consequence, if k is a reconstruction kernel, $k*P_{\theta}f$ is constant on $(-a, a)$ except near the ends, has negative dips at the ends, and goes rapidly to 0 outside $(-a, a)$; the convolution converts elliptical features along a line of the radiograph into rectangular features, alleviating the three problems mentioned above. A weighted average of the original and the convolution contains both the sharpened features of the latter and the overall features of the former, but in a decreased dynamic range, and with dips at the edges. The effect of the convolution on ellipses is shown in Fig. 1.

As an approximation to the operator Λ , which entails both differentiation and singular integration, convolution by k creates a noise explosion, as shown in Fig. 2.

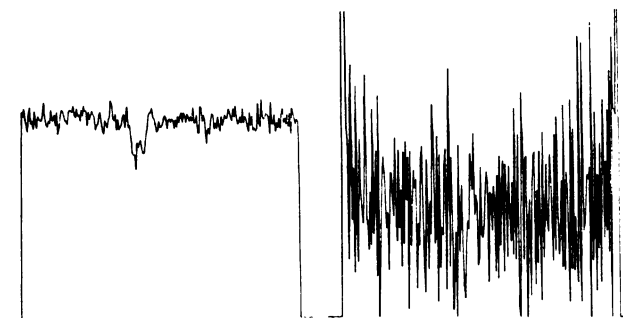


FIG. 2. Noise explosion. The function g (Left) is the top part of a line across a radiograph of a 0.01-inch steel shim, sandwiched in a 0.25-inch steel plate. The central dips come from two 0.02-inch diameter holes in the shim, 0.01 inch apart. Other oscillations are noise. (Right) The function is $0.5g + 0.5k*g$.

Noise Elimination

Depending on the measurement devices and the nature of the problem, the signal-to-noise ratio on radiographs can be quite small—on the order of 1/10th in the case of medical x-ray film and soft tissue discrimination. In earlier work (1), a provisional noise elimination procedure was devised for situations in which the signal-to-noise ratio is very small, but the true signal is known *a priori* to be smooth, except perhaps for jumps. The idea of the procedure was to correct in several steps. In the early steps, when good corrections are impossible, changes are made only at the worst points; as the data improve, changes are made more often.

The procedure eliminates noise from a function g of one variable that is known to be smooth except for jumps. At a given stage, there are fixed an interval length L and a noise bound N . For each point x , the medians of g are computed on the intervals $(x - L, x)$, $(x, x + L)$, and $(x - L, x + L)$. If they are denoted by $M_l(x)$, $M_r(x)$, and $M(x)$, the noise $N(x)$ is defined to be the minimum of $|g(x) - M_l(x)|$, $|g(x) - M_r(x)|$, $|g(x) - M(x)|$. If $N(x)$ exceeds the bound N , then $g(x)$ is replaced by $M(x)$; otherwise, it is left alone. The bound N is chosen so that in the first and second steps corrections are made at 2% of the points, in the third and fourth steps at 4% of the points, in the fifth at 12% of the points, in the sixth at 25% of the points, and in the seventh (and last) at all the points, with averages instead of medians. The interval lengths are 8, 8, 6, 4, 3, 2, and 2 in the seven steps. In problems without severe noise, the number of steps and the interval lengths are decreased.

This procedure has been used in x-ray tomography, ultrasound tomography, and the analysis of individual radiographs produced by x-ray and neutron beams. Some examples are found in ref. 1, and a detailed example showing the operation of the procedure and the effect at each stage is given in ref. 4. The noise elimination operator is called S .

The Sharpening Operator

The sharpening operator combines convolution with a CT kernel and the smoothing operator S to control the noise and the dips at edges. If $g = P_0 f$ is a function of two variables, let Sg and $k*g$ denote the result of applying the smoothing and convolution to g as a function of the first variable with the second held fixed, and let $g^*(x, y) = g(y, x)$. Usually, the sharpening operator is given by

$$\text{Sharp } g = w_1 g + w_2 k*Sg + w_3 (k*Sg^*)^*, \quad [2.1]$$

cut off below, with weights based on the flattening needed. Effects of the sharpening operator are shown in Fig. 3.

Examples

Being flat already, the shim and CT sections shown in Figs. 4 and 5 are poor candidates for the sharpening process, but

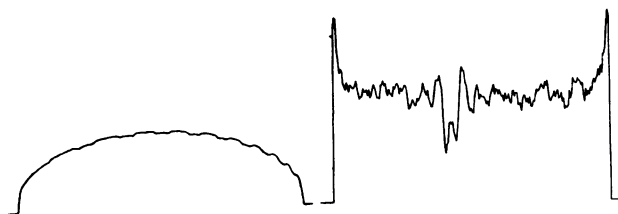


FIG. 3. Effect of the sharpening operator. The functions shown are Sharp $g = 0.5g + 0.5k*Sg$. (Left) g is the bumpy ellipse; (Right) g is the shim.

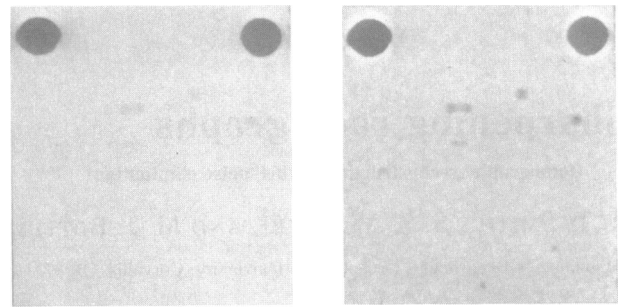


FIG. 4. Sandwiched shim of Figs. 2 and 3. Among the several holes (black spots), there are three pairs in a column to the left of the center with distances apart of 0.01 inch and diameters of 0.04, 0.02, and 0.01 inches. Sharp g (Right) = $0.5g + 0.25k*Sg + 0.25(k*Sg^*)^*$.

they do have some relevance. The shim gives an indication of the resolution of the process. The CT section shows what happens to a more complex flat image and, also, the result of another current sharpening technique called temporal subtraction. Figs. 6–8 show a jet engine blade, a low-contrast phantom, and a human chest, respectively.

Discussion

Early use of simple mathematics to isolate local features (breast lesions) from the background appeared in ref. 5.

In the mid 1970s, J. Kinsey tried (personal communication) $k*g$ as an edge detector similar to differentiation. The convolution has a more specific effect than differentiation in the case of radiographs, but consistent results appear to require the noise elimination and averaging with the original. In some cases, however, omission of the noise elimination

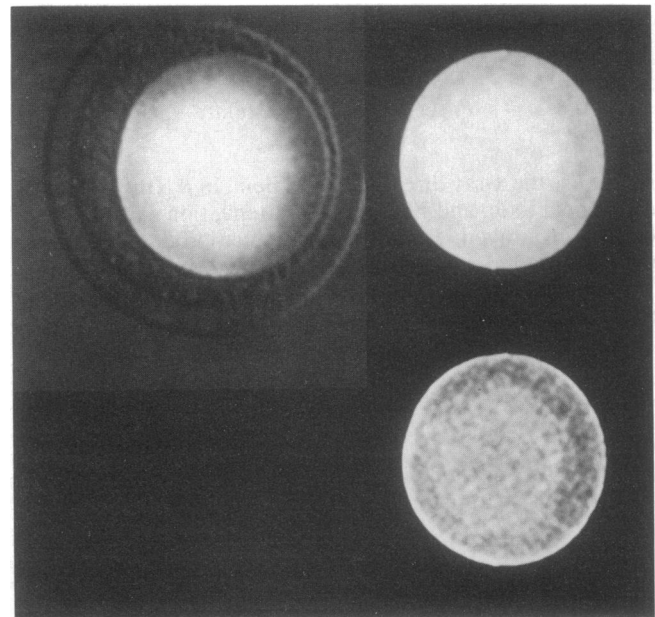


FIG. 5. Oil flow through rock. To study the flow of oil through rock, CT sections are taken before the flow and as it progresses, and corresponding sections are subtracted. A subtraction is shown (Upper left), and a single section is shown (Upper right), with the sharpened version of it (Lower right). Subtracted sections are matched within one pixel, but subtraction artifacts are apparent in the exterior of the rock and in the loss of the fine structure. High densities (white) are due to sodium iodide in the water forcing the flow.

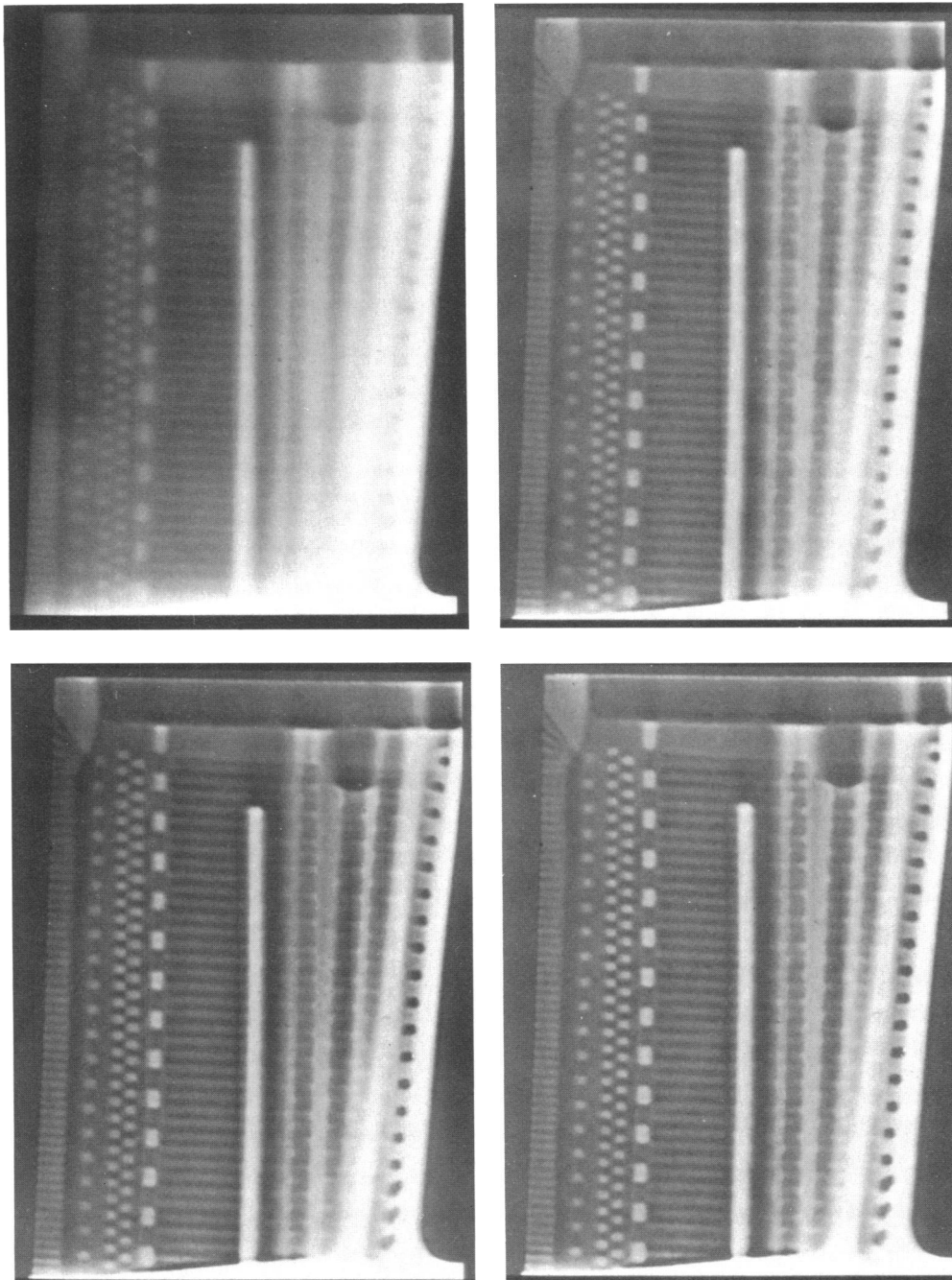


FIG. 6. Jet engine blade. (Upper left) Original = g . (Upper right) $0.3g + 0.35k*Sg + 0.35(k*Sg^*)^*$. (Lower left) $0.1g + 0.45k*Sg + 0.45(k*Sg^*)^*$. (Lower right) $0.5k*Sg + 0.5(k*Sg^*)^*$. The short dark horizontal lines on the left edge of the blade are holes. The sharpened images show an apparent abnormality in the fourth hole, which can be confirmed in the original by extreme windowing that whites out the rest of the image. The nature of the abnormality is not known.

can be useful in exaggerating fine lines or single pixels in the digital radiograph (possibly coming from fine cracks or microcalcifications). In other cases, omission of the original can be useful.

During the final preparation of this manuscript the article of Kalender *et al.* (6) appeared with a method for sharpening radiographs by decreasing global variations. The sharpening operator in ref. 6 is given by Sharp $g = w_1g + w_2(1 - S_2)g$, where S_2 is a 2-dimensional convolution smoothing operator. Global features of g are preserved by S_2 , therefore, killed by $1 - S_2$. Since all features preserved by S_2 are killed by $1 - S_2$, the choice of S_2 is dependent on the object x-rayed and the particular features to be visualized.

In the present method, the sharpening operator is the same in all cases (e.g., jet engine blade, phantom, and chest-radiographs of very different natures) with the possibility of varying the weights for different degrees of flattening.

As shown by the shim in Fig. 4, the spatial resolution of the sharpened radiograph is about equal to that of the original. A primary factor in the spatial resolution of digital radiographs is the x-ray beam collimation. In the case of the shim and engine blade, the collimation was 0.005 inches wide and 0.010 inches high; in the case of the chest it was 0.7 mm wide and 1.9 mm high. With moving objects, the scan time is a factor. In the case of the chest, the scan time was about 5 sec.

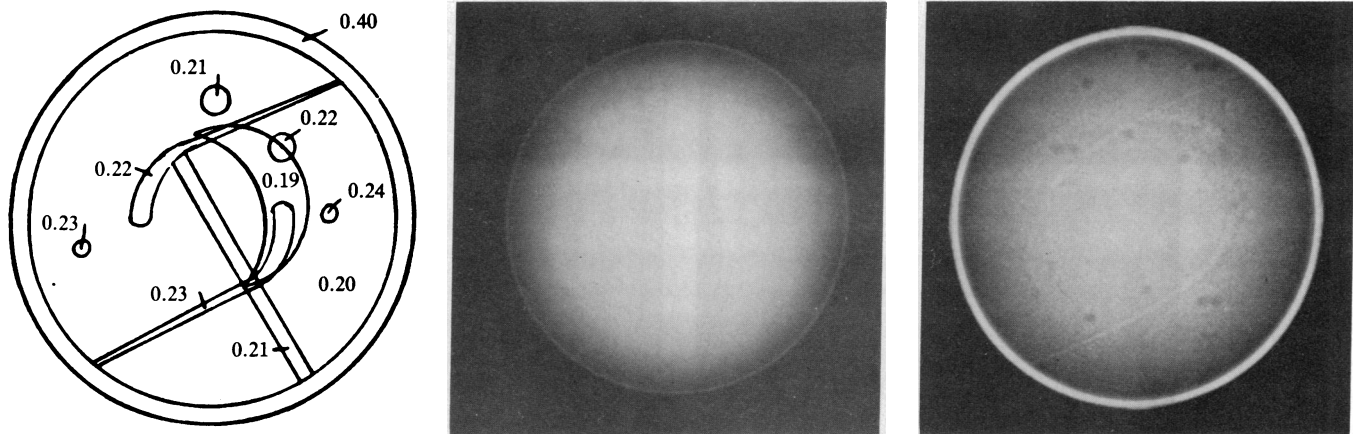


FIG. 7. Low-contrast phantom. The mathematical phantom is an ellipsoid with a heavy outer shell and interior features with attenuation coefficients shown in the sketch and circular horizontal cross-sections. The interior background has a coefficient of 0.20. To provide real noise and some odd variations, the middle part of the shim of Fig. 4, normalized to a mean value of 0 and scrambled, is added. With attenuation values on the scale 0–10,000, the maximum positive value in the normalized shim is 123; the average positive value is 18. These represent the maximum and average values of the noise, as negative shim values include the holes, where the minimum is about –400. The attenuation change across the lightest “artery” is 13; along the central horizontal line, attenuation is 9605 and 9607 to the left and right of the artery, respectively, and 9618 at the middle. Note that even the shim holes with a variation of 400 are not seen in the original. Sharp $g = 0.3g + 0.35k*Sg + 0.35(k*Sg)^*$. This is a combined real and mathematical radiograph, not a cross-section.

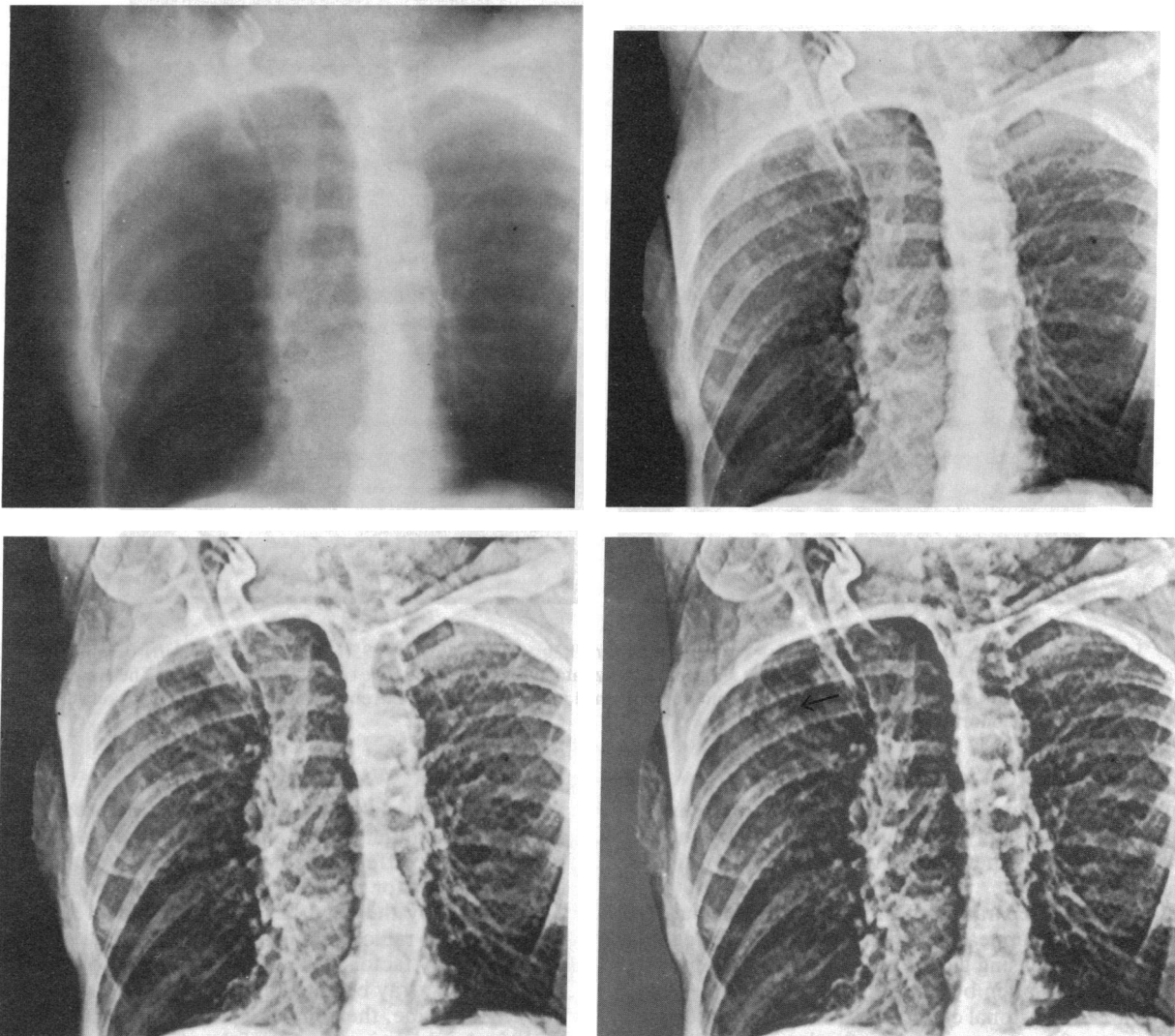


FIG. 8. Chest, oblique view. (Upper left) Original = g . (Upper right) $0.3g + 0.35k*Sg + 0.35(k*Sg)^*$. (Lower left) $0.1g + 0.45k*Sg + 0.45(k*Sg)^*$. (Lower right) $0.5k*Sg + 0.5(k*Sg)^*$. At the arrow, a CT body scan showed a small ill-defined region of increased density, which was not seen, even in retrospect, on unsharpened individual radiographs. After 1.5 yr, nothing of clinical significance has developed.

This research was supported by National Science Foundation Grant MCS-8101586, by equipment grants from the Cromemco and Tektronix Companies, and by the General Electric Visiting Research Fellowship Program.

1. Smith, K. T., Solmon, D. C. & Wagner, S. L. (1977) *Bull. Am. Math. Soc.* **83**, 1227–1270.
2. Ramachandran, G. N. & Lakshminarayanan, A. V. (1971) *Proc. Natl. Acad. Sci. USA* **68**, 2236–2240.
3. Logan, B. F. & Shepp, L. A. (1974) *IEEE Trans. Nucl. Sci.* **21**, 21–43.
4. Smith, K. T. (1983) *Iterative Noise Elimination* (Mathematics Research Center, Univ. of Wisconsin, Madison), Tech. Rep. 2464.
5. Smith, K. T., Wagner, S. L., Guenther, R. B. & Solmon, D. C. (1977) *Radiology* **125**, 383–386.
6. Kalender, W., Hubener, K. & Jass, W. (1983) *Radiology* **149**, 299–303.